

DEVELOPMENT AND VERIFICATION OF AN ALGORITHM FOR
 HELICOPTER INVERSE SIMULATIONS

D.G. THOMSON and R. BRADLEY

Department of Aerospace Engineering
 University of Glasgow
 Glasgow

Abstract - The control displacements required for a helicopter to fly a defined manoeuvre may be calculated by inverse solution of the vehicle's equations of motion. A computer package, HELINV, has been developed to perform such solutions, or inverse simulations, for a series of nap-of-the-earth (NOE) manoeuvres. This gives a unique opportunity to study simulated control strategies in constrained flight. The algorithm, described in this paper, uses a six degrees of freedom nonlinear mathematical model which allows solutions to be found for various helicopter configurations flying a wide range of manoeuvres. Some typical results are presented, along with a discussion of the limitations and potential applicability of the algorithm. The method is verified by use of time response calculations. In addition, flight data is used to validate the results of inverse simulations.

NOMENCLATURE

b	= number of blades	$\ddot{x}, \ddot{y}, \ddot{z}$	= acceleration components along x,y,z earth fixed axes
C_Q	= main rotor torque coefficient	x_{CG}	= centre of gravity position fwd. of fuselage ref. pt.
C_T	= main rotor thrust coefficient	β	= fuselage sideslip angle
C_{Ttr}	= tail rotor thrust coefficient	β_{1c}	= main rotor longitudinal flapping angle
g	= acceleration due to gravity	β_{1s}	= main rotor lateral flapping angle
h	= altitude	γ	= angle of climb
h_R	= height of main rotor hub above fuselage ref. point	γ_s	= forward tilt of rotor shaft
h_{tr}	= height of tail rotor hub above fuselage ref. point	δ	= main rotor profile drag coefficient
I_{xx}, I_{yy}, I_{zz}	= moments of inertia	θ	= fuselage pitch attitude angle
I_{xz}	= product of inertia	θ_0	= main rotor collective pitch angle
L, M, N	= external rolling, pitching and yawing moments	θ_{1c}	= main rotor lateral cyclic pitch angle
L_A, M_A, N_A	= external aerodynamic moments	θ_{1s}	= main rotor longitudinal cyclic pitch angle
l_{tr}	= tail rotor distance from fuselage reference point	θ_{otr}	= tail rotor collective pitch angle
K_β	= blade flapping stiffness	μ_x, μ_y, μ_z	= normalised components of rotor hub velocity
m	= helicopter mass	ρ	= density of air
p, q, r	= roll, pitch and yaw rates	σ	= solidity of main rotor
R	= main rotor radius	ϕ	= fuselage roll attitude angle
R_{tr}	= tail rotor radius	x	= track angle
s	= distance along track	ψ	= fuselage yaw attitude angle
t	= time	Ω	= main rotor speed
u, v, w	= translational velocities along the x,y,z body axes	Ω_{tr}	= tail rotor speed
V	= flight velocity		
\dot{V}	= flight acceleration		
X, Y, Z	= external forces along the x, y, z body axes		
X_A, Y_A, Z_A	= aerodynamic external forces		
$\dot{x}, \dot{y}, \dot{z}$	= velocity components along x,y,z earth fixed axes		

1. INTRODUCTION

In conventional simulation it is possible to compare the responses of different aircraft configurations to a set control sequence. In general, different flight paths will result, and these can provide a measure of the effect of configurational changes. An alternative method of assessment, which requires inverse solutions of the aircraft equations of motion, is to compare the control sequences necessary to follow a defined flight path. This makes inverse methods particularly useful when studying helicopter performance during tightly defined manoeuvring flight, such as in NOE missions or air-to-air combat manoeuvres. There is much current interest in structuring missions in terms of MTE's (Mission Task Elements) [1, 2] in the context of revising the MIL-H-8501 [3] handling qualities criteria. Clearly inverse simulation is a fundamental technique of such an exercise.

Most attempts at solving aircraft equations of motion inversely have been based on simulations of fixed wing aircraft. Some of the first attempts used very basic low order linearised models, for example Jones [4] used an analytic technique to solve inversely the equations of motion to study gust effects. As mathematical models grew more complex inverse solutions became more difficult to achieve by analytical methods, and it is only recently, with the increased availability of powerful computing facilities able to calculate numerical solutions, that flight dynamicists have renewed their interest in inverse methods. In addition, control system designers have found inverse methods useful in the development of Automatic Flight Control Systems, the work by Meyer and Cicolani [5] being a good example. Kato and Sugiura [6] have developed a more general method for fixed wing aircraft which, in theory, should allow them to compute control and state time histories for a general commanded flight path (although the only example they cite is a straight and level flight path with a continuous 360 degree roll imposed on it). Although similar to the method described in this paper, Kato and Sugiura use fuselage attitude time histories as the starting point of their solution rather than specifying a flight path directly.

Few attempts have been made to solve helicopter equations of motion inversely. A recent attempt by Houston and Caldwell [7] used a reduced order linearised model of a helicopter's longitudinal dynamics to study the use of an active tailplane in longitudinal manoeuvring flight. The method used relies on a linearised mathematical model and hence suffers from the restriction of being valid only for small perturbations from the trim state. The inverse method described herein uses a nonlinear six degrees of freedom mathematical model, and so has no restriction on the allowable displacement from trim. The starting point for the solution is a precisely defined flight path, and this flight path may be "flown" with any number of configurations. The package HELINV is a FORTRAN implementation of the inverse algorithm.

2. INVERSE SIMULATION : A DECLARATION OF THE PROBLEM

The solution procedure for the inverse method is best appreciated from the stand point of the influence of the control movements on the dynamics of the helicopter. It is helpful therefore to start by examining the basic equations of motion.

2.1 The Basic Equations

A conventional helicopter simulation involves solution of the six nonlinear equations of motion (1) for the six unknown state variables: u, v, w , the translational velocities, and p, q, r the angular velocities, in a body-fixed frame of axes (see Figure 1).

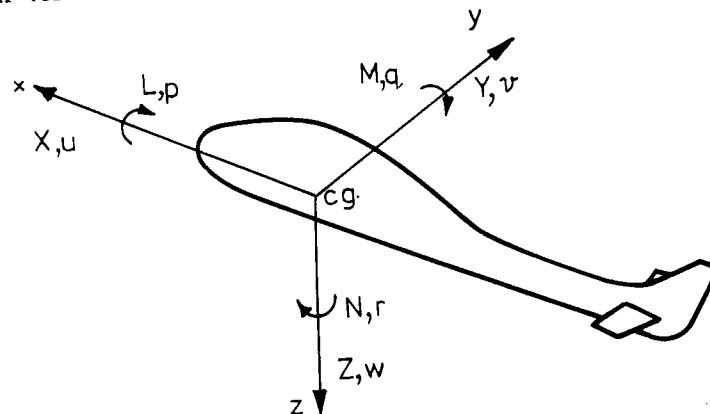


Figure 1 : Body Fixed Axes System

$$m\dot{u} = -m(wq - vr) + X - mg \sin\theta \tag{1.1}$$

$$m\dot{v} = -m(ur - wp) + Y + mg \cos\theta \sin\phi \tag{1.2}$$

$$m\dot{w} = -m(vp - uq) + Z + mg \cos\theta \cos\phi \tag{1.3}$$

$$I_{xx} \dot{p} = (I_{yy} - I_{zz})qr + I_{xz}(r^2 + pq) + L \tag{1.4}$$

$$I_{yy} \dot{q} = (I_{zz} - I_{xx})rp + I_{xz}(r^2 - p^2) + M \tag{1.5}$$

$$I_{zz} \dot{r} = (I_{xx} - I_{yy})pq + I_{xz}(\dot{p} - qr) + N \tag{1.6}$$

The helicopter's attitude angles (θ, ϕ, ψ) are Euler angles relating the body fixed frame to an earth fixed frame of reference, and are found by solving the kinematic relations:

$$\dot{\phi} = p + q \sin\phi \tan\theta + r \cos\phi \tan\theta \tag{2.1}$$

$$\dot{\theta} = q \cos\phi - r \sin\phi \tag{2.2}$$

$$\dot{\psi} = q \sin\phi \sec\theta + r \cos\phi \sec\theta \tag{2.3}$$

For a conventional helicopter the rotor controls are $\theta_0, \theta_{1s}, \theta_{1c}$ which are, respectively, the collective, longitudinal cyclic and lateral cyclic angles of pitch of the blades. The collective angle of the tail rotor blades is θ_{otr} . These determine the main rotor thrust and its direction through the thrust coefficient C_T , and the angles of flap β_{1s} and β_{1c} (illustrated in Figure 2), and also the tail rotor thrust through its coefficient C_{Ttr} . The values of the external forces X, Y, Z and moments L, M, N are derived from $C_T, \beta_{1s}, \beta_{1c}$ and C_{Ttr} (see equations 3).

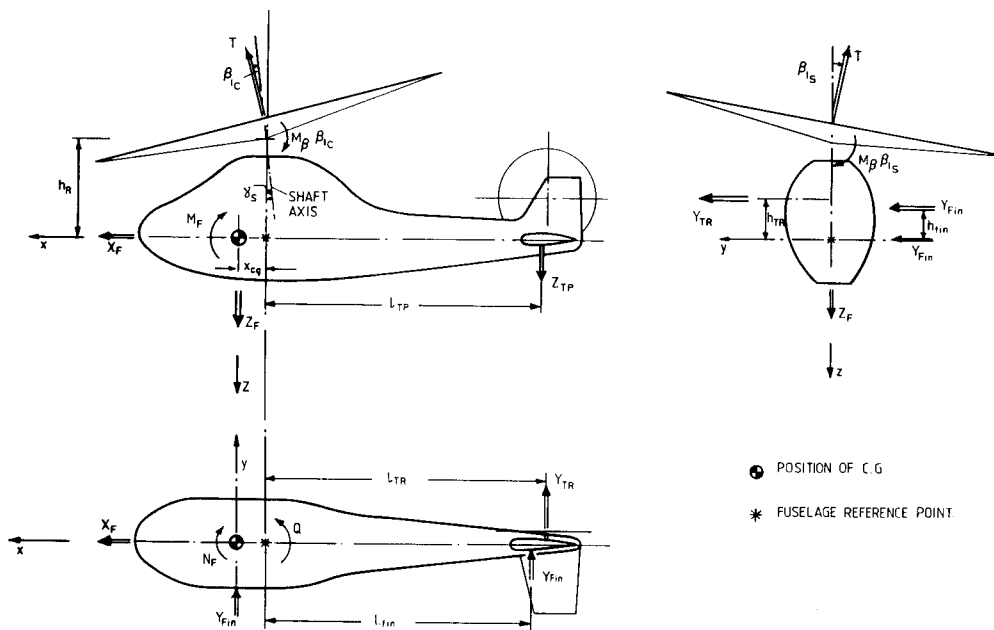


Figure 2 : Components of External Forces and Moments on a Conventional Helicopter

2.2 Method of Solution

Once a forward solution based on a standard time stepping method is available, the inverse solution appears to be a straight forward development. At each new time increment the values of the rotor control angles must be varied to ensure that the correct flight path is achieved. Expressing the accelerations and rates in discrete form reduces the problem to the solution of a set of algebraic equations at each time increment. The equations may be solved globally over the whole range of integration simultaneously or incrementally as the solution develops. A unique inverse solution is usually guaranteed by imposing an additional constraint in the form of a specified heading or sideslip angle. The problem lies in the difficulty of solving the equations in a reliable way for a representative range of flight paths once mathematical models of any complexity are employed. Standard black box

techniques prove to be inefficient and some understanding of the underlying flight mechanics is needed to establish a solution procedure which can form the basis of a useful tool. Therefore in an inverse method there are three elements. One is the mathematical model to be used, another is the set of flight paths to be considered, and finally there is the structure of the inverse solution algorithm. They are considered in the following sections: 3.1 to 3.7.

3. THE "HELINV" INVERSE SIMULATION ALGORITHM

The HELINV numerical algorithm is now discussed, a more detailed description is given by Thomson [8]. The algorithm is shown schematically in Figure 3.

3.1 The Mathematical Model

The accuracy and validity of any form of solution of the equations of motion depends on the mathematical model used. There are always advantages to be gained by making a model as tractable as possible both in the understanding of the problem, and in computational time. However, simple mathematical models have limitations which preclude their use in inverse analyses. The limitations of using kinematic models, as discussed by Curtiss and Price [9], are poor prediction of dynamic behaviour at low speed, whilst reduced order dynamic models have the problem of poor (if any) prediction of coupling effects when simulating hingeless rotor helicopters. Linearised models are also of limited use since they only predict the helicopter's flight state for small disturbances from its trim condition. Use of any of the models mentioned above would impose limitations on the severity of the manoeuvres over which valid inverse solutions could be found.

Work at Glasgow University on inverse solutions has been supported by the Royal Aerospace Establishment who made available their own mathematical model for the study of helicopter flight mechanics. This model forms the basis of the simulation package "HELISTAB"; a detailed description of the modelling of the forces (X,Y,Z) and the moments (L,M,N) is given by Padfield [10]. HELISTAB is an established mathematical model capable of simulating single main and tail rotor helicopters, and has undergone many improvements over several years. An early version, HELISTAB2, has been incorporated into the HELINV package. This is a six degrees of freedom, nonlinear model. Some of the main features of this model are:

- i) Rotor blades are assumed to be rigid, to be of constant chord, and to have constant lift curve slope.
- ii) The flow around the blades is assumed to be steady and incompressible.
- iii) Stall and reversed flow effects are ignored.
- iv) A centre spring representation of the rotor is used to simulate the flapping behaviour of the blades.
- v) Quasi-steady flapping and coning is assumed.
- vi) Fuselage, tailplane and fin aerodynamic loads are calculated from empirically derived expressions.

The external forces and moments for the equations of motion (1) are then given by the following expressions.

$$X = X_A + \rho(\Omega R)^2 \pi R^2 [C_T (\beta_{1c} + \gamma_s) - \delta\sigma\mu_x/4] \quad (3.1)$$

$$Y = Y_A + \rho(\Omega R)^2 \pi R^2 [-C_T \beta_{1s} - \delta\sigma\mu_y/4] + \rho(\Omega_{tr} R_{tr})^2 \pi R_{tr}^2 C_{Ttr} \quad (3.2)$$

$$Z = Z_A - \rho(\Omega R)^2 \pi R^2 C_T \quad (3.3)$$

$$L = L_A - b/2 K_B \beta_{1c} + \rho(\Omega R)^2 \pi R^2 h_R [-C_T \beta_{1s} - \delta\sigma\mu_y/4] + \rho(\Omega_{tr} R_{tr})^2 \pi R_{tr}^2 h_{tr} C_{Ttr} \quad (3.4)$$

$$M = M_A - [b/2 K_B \beta_{1c}] - \rho(\Omega R)^2 \pi R^2 [h_R C_T (\beta_{1c} + \gamma_s) - h_R \delta\sigma\mu_x/4 - x_{cg} C_T] \quad (3.5)$$

$$N = N_A + \rho(\Omega R)^2 \pi R^3 C_Q + \gamma_s [-b/2 K_B \beta_{1s} + \rho(\Omega R)^2 \pi R^2 h_R (-C_T \beta_{1s} - \delta\sigma\mu_y/4)] - (l_{tr} + x_{cg}) \rho(\Omega_{tr} R_{tr})^2 \pi R_{tr}^2 C_{Ttr} \quad (3.6)$$

where X_A N_A are the aerodynamic forces and moments, composed of components from the fuselage, fin and tail surfaces.

3.2 Defining Manoeuvres

The success of an inverse simulation depends to a large degree on the ability to define realistic manoeuvres. The flight paths modelled in HELINV were chosen, in collaboration with the Royal Aerospace Establishment, Flight Management Department to represent tasks frequently flown in NOE conditions, including manoeuvres for which flight test data was available. A manoeuvre is defined as a time history of the helicopter's

k = k +

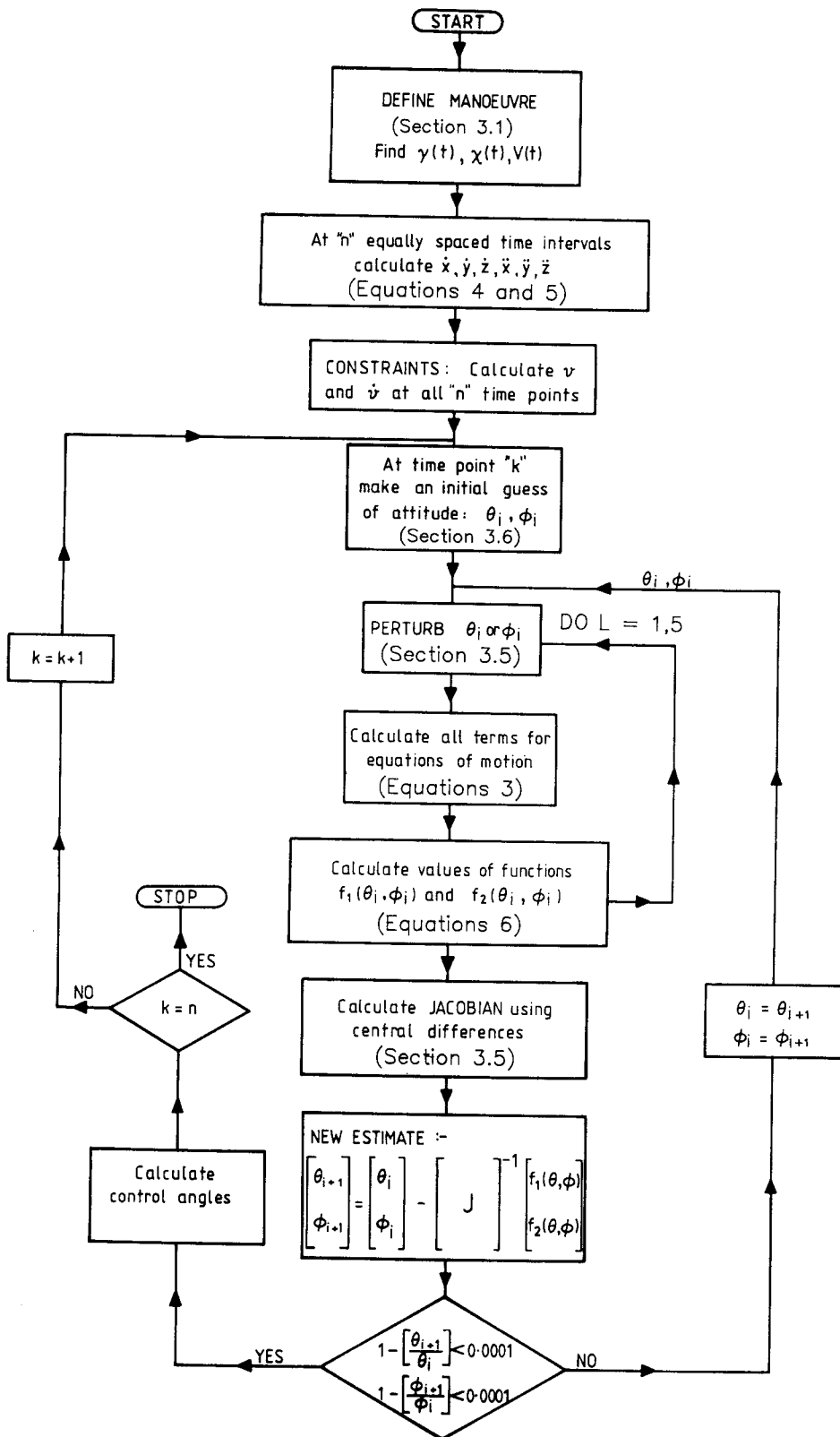


Figure 3 : Flowchart of Inverse Algorithm

earth-axis velocities and accelerations. Since numerical differentiation is used to calculate attitude rates at points throughout the manoeuvre, these velocities and accelerations are most conveniently calculated at a series of equally spaced time intervals. Referring to Fig. 4 it is apparent that the components of velocity in the earth axes system are given by :

$$\dot{x} = V \cos \gamma \cos \alpha \tag{4.1}$$

$$\dot{y} = V \cos \gamma \sin \alpha \tag{4.2}$$

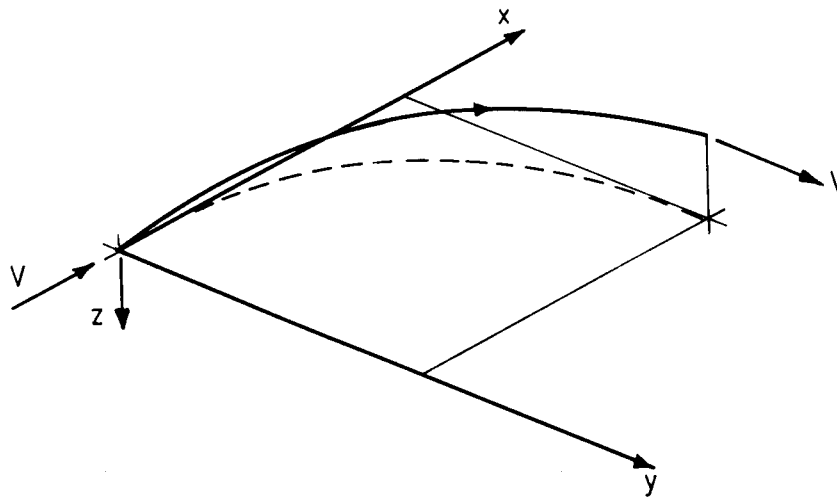
$$\dot{z} = -V \sin \gamma \tag{4.3}$$

and the accelerations are found to be, by differentiation:

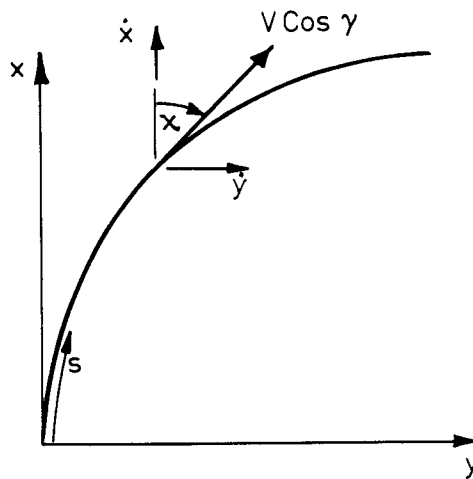
$$\ddot{x} = \dot{V} \cos \gamma \cos \alpha - V \dot{\gamma} \sin \gamma \cos \alpha - V \dot{\alpha} \cos \gamma \sin \alpha \tag{5.1}$$

$$\ddot{y} = \dot{V} \cos \gamma \sin \alpha - V \dot{\gamma} \sin \gamma \sin \alpha + V \dot{\alpha} \cos \gamma \cos \alpha \tag{5.2}$$

$$\ddot{z} = -\dot{V} \sin \gamma - V \dot{\gamma} \cos \gamma \tag{5.3}$$



a) The Flight Path



b) The Track

Figure 4 : A General 3-Dimensional Manoeuvre

Manoeuvres
example) as
it (Fig. 4c
functions of
a specified
wing-over.
to define f

3.3 Sideslip

If
apply four
Defining th
constraints
controls :
the y-dire
constraint
most appro
sideslip or
may be dep
zero sidesl
may be mor
of freedom
for example
or heading

When sidesl

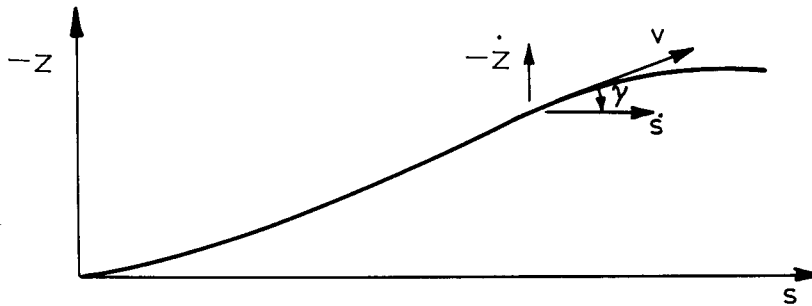
and

In the h
differentia

3.4 The T

A t
flight stat
equations a

Modifi
would allow
simulation
the simula
iterative



c) The Altitude

Manoeuvres are defined by considering a three dimensional flight path (Figure 4a, for example) as a track in the xy plane (Fig. 4b), with an altitude variation superimposed on to it (Fig. 4c). The flight velocity V , climb angle γ , and track angle α are then specified as functions of time. The manoeuvres available include: pop-up, a height change performed over a specified distance, bob-up, a vertical height change, accelerated/decelerated turns, and wing-over. Full descriptions of the current range of manoeuvres, and the algorithms used to define flight paths are given by Thomson [11].

3.3 Sideslip and Heading Constraints

If a unique solution of the equations of motion is to be found it is necessary to apply four constraints on the helicopter's motion (corresponding to the four controls). Defining the flight path as a function of time (equations (4) and (5) above), gives three constraints. These can be considered, in simplistic terms, as corresponding to the three controls: longitudinal cyclic controlling displacements in the x-direction, lateral cyclic the y-direction and collective the z-direction. It follows that the choice of fourth constraint should be related to the influence of the tail rotor collective control. The most appropriate form of constraint is therefore one applied to either the helicopter's sideslip or heading angles, the choice being left to the user of the program. This choice may be dependent on the task to be simulated, for example it may be desirable to apply a zero sideslip constraint to produce a co-ordinated turn, whilst a zero heading constraint may be more appropriate for a rectilinear manoeuvre. In NOE flight, control of this degree of freedom is important not only for the pilot's vision, but also for fuselage; pointing, for example, large angles of sideslip are often used to decelerate the helicopter. Sideslip or heading angles can be expressed as a functions of time:

$$\beta = \beta(t) \quad \text{or} \quad \psi = \psi(t)$$

When sideslip is to be constrained, the sideslip velocity and acceleration are given by :

$$v = V \sin\beta \quad (6)$$

and

$$\dot{v} = \dot{V} \sin\beta + \beta V \cos\beta \quad (7)$$

In the heading constrained case, yaw rate and acceleration are found simply by differentiation of the defining function.

3.4 The Trim Algorithm

A trim algorithm calculates the control angles needed to maintain a defined steady flight state. It can therefore be considered as a basic form of inverse solution. The trim equations are obtained by setting the the inertial terms to zero in equations (1) so that

$$X - mg \sin\theta = 0 \quad (8.1)$$

$$Y + mg \cos\theta \sin\phi = 0 \quad (8.2)$$

$$Z + mg \cos\theta \cos\phi = 0 \quad (8.3)$$

$$L = M = N = 0 \quad (8.4)$$

Modification of equations (8) to include the acceleration and inertial terms as in (1) would allow a trim algorithm to find inverse solutions for manoeuvring flight. A forward simulation algorithm usually includes a trim algorithm in order to give a smooth start to the simulation. The HELISTAB simulation incorporates a trim algorithm which uses nested iterative loops, with simple successive substitution, to solve equations (7) for the

fuselage attitude angles θ, ϕ , the main and tail rotor thrust coefficients C_T, C_{Ttr} , and the longitudinal and lateral flapping angles β_{1c}, β_{1s} . As well as being expensive in computer time, this solution was very sensitive to initial condition, and numerically unstable when solving for turning flight. For these reasons, when the trim algorithm was modified to include acceleration and inertial forces and moments, it was also restructured to allow solution using a faster, and more reliable Newton-Raphson iterative scheme.

3.5 Solution Using a Newton-Raphson Iteration

The solution is obtained by an iteration on the two attitude angles θ and ϕ . Starting with initial values for these angles at each time step there is a natural evolution of the solution procedure. It is important to appreciate the mechanism by which the helicopter is controlled. The dominant component of the main rotor thrust acts, through the force Z , in a direction colinear with the z axis, and the direction of this axis is determined, since it is body fixed, by rotations about the three axes effected by the moments L, M and N . Now the force Z is controlled by the thrust coefficient C_T (equation 3.1), and then L, M and N are controlled respectively by the angles of flap β_{1s}, β_{1c} (equations 3.4-3.6) and the tail rotor thrust coefficient C_{Ttr} . With this knowledge it is clear that the w, p, q , and r equations of motion, equations (1.3-1.6), must be used to solve for $C_T, \beta_{1s}, \beta_{1c}$ and C_{Ttr} (by incorporating equations 3.3-3.6). In the current models, if all other terms are known, these four equations effectively become linear and are easily solved for the above parameters. It is then possible to calculate X and Y in the first two of equations (1), which are written in the form

$$F_1(\theta, \phi) = -m(\dot{u} + wq - vr) + X - mg \sin\theta = 0 \quad (9.1)$$

$$F_2(\theta, \phi) = -m(\dot{v} + ur - wp) + Y + mg \cos\theta \sin\phi = 0 \quad (9.2)$$

The calculation of the other quantities in F_1 and F_2 is discussed in section 4.7.

At a point, i , in the iteration, the next estimate of the solution is given by:

$$\begin{bmatrix} \theta_{i+1} \\ \phi_{i+1} \end{bmatrix} = \begin{bmatrix} \theta_i \\ \phi_i \end{bmatrix} - \begin{bmatrix} \frac{\partial F_1}{\partial \theta} & \frac{\partial F_1}{\partial \phi} \\ \frac{\partial F_2}{\partial \theta} & \frac{\partial F_2}{\partial \phi} \end{bmatrix}^{-1} \begin{bmatrix} F_1(\theta_i, \phi_i) \\ F_2(\theta_i, \phi_i) \end{bmatrix} \quad (10)$$

where the partial derivatives are calculated by numerical differentiation with fractional changes of 0.0001 in the angles θ and ϕ .

3.6 Initial Guesses of Attitude Angles

The inverse solution was found to be very sensitive to initial value. This sensitivity is directly related to the severity of the manoeuvre, that is as the manoeuvre becomes more severe, the difference in the values of the attitude angles between successive time steps increases, hence better first guesses were required. A cubic polynomial function is fitted through the previous five points in the θ and ϕ time histories, better initial values are then found by extrapolation. This reduces computing time by ensuring rapid convergence. Over the first few time points, where there are too few points to fit a polynomial, the initial guesses are found by linear extrapolation.

3.7 Calculation of Functions F_1 and F_2

The functions F_1 and F_2 must be evaluated using the latest estimates θ and ϕ within the iterative scheme. This involves calculation of body axes velocities and accelerations as well as the external (aerodynamic and rotor) forces and moments. The process used to achieve this is now presented.

3.7.1 Calculation of Yaw Angle and Rate

As mentioned in section 3.3, either heading or sideslip angle must be defined if a unique solution is to be found. It is also apparent that if the sideslip constraint is chosen, then it becomes necessary to find the corresponding heading angle in order to compute the body axes velocities from the predefined earth axes values. The yaw angle ψ and its rate are found from the known values of sideslip velocity and acceleration (equations 5 and 6), and by using the transformation from earth to body axes. Transformation from earth to body axes (or vice versa) is achieved by use of the Euler transformation. Thus body axes velocities are found from earth axes velocities by using the direction cosine matrix :

study
follow

4.1

helico
the f
been
The f
second
rotor
stiff
eviden

whils
hurdl
flown
attit
displ
signi
plots
the
towar
Longi
forwa
the
Fusel
also
oppos
Lynx.

4.2

confi
is s
speci
turni
secti
the f
to be
diffe
cont
sever
manoe

4. SOME EXAMPLES OF "HELINV" INVERSE SIMULATIONS

The inverse simulation package, HELINV, was developed initially for use in an agility study [8], but there are many other potential uses. Two such uses are described in the following sections.

4.1 Configurational Studies

The power of an inverse method is its ability to simulate any number of types of helicopters flying a precisely defined and repeatable manoeuvre. This is demonstrated by the following set of results obtained from HELINV. Two sets of configurational data have been used in the mathematical model to represent two completely different helicopter types. The first set of data is used to simulate the Westland Lynx battlefield helicopter, and the second set of data represents a Aerospatiale Puma transport configuration. The semi-rigid rotor of the Lynx should give much greater control power (due to its higher flapping stiffness) than the articulated rotor of the Puma. This fundamental difference should be evident on the control time histories calculated by HELINV.

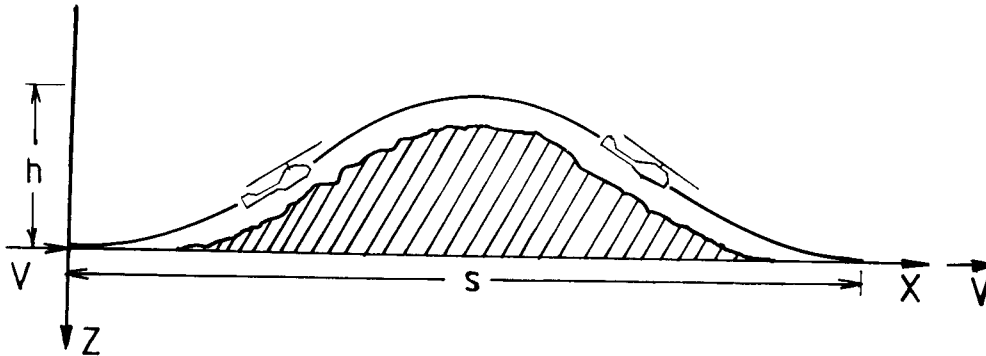


Figure 5 : The Hurdle-Hop Manoeuvre

A hurdle-hop (Figure 5) is a terrain following manoeuvre used to evade detection whilst avoiding obstacles at low level in nap-of-the-earth flight. In this example, the hurdle height, h , is 25m and the manoeuvre distance, s , is 500m. The whole manoeuvre is flown at a constant speed of 80 knots, and with sideslip constrained to be zero. The attitude and control time histories of both aircraft are plotted in Figure 6 as displacements from their trim values. As expected the plots show the Lynx requires significantly smaller control displacements to fly the same manoeuvre than the Puma. The plots show main rotor collective pitch which controls the helicopter's height, positive in the climbing phase until the hurdle is cleared, then negative as the aircraft descends towards the exit. It then becomes positive again as the helicopter levels off. Longitudinal cyclic pitch which is used to control forward speed, is negative (indicating a forward tilt of the rotor thrust vector) in the climb phase of the manoeuvre and positive in the descent. This is a consequence of constraining the helicopter's speed to be constant. Fuselage pitch attitude is influenced both by the displacements in longitudinal cyclic, and also by the geometry of the flight path. Lateral cyclic and roll angle, ϕ , plots indicate opposite trends since the rotor of Puma rotates in the opposite direction to that of the Lynx.

4.2 Manoeuvre Studies

It is also possible using inverse simulation to compare the performance of a single configuration flying a series of manoeuvres. In the following example the Lynx helicopter is simulated flying a series of level turns of various radii. Turns are defined by specifying turn rate as a function of time [11]. This allows the transition from linear to turning flight to be simulated. In this example, the manoeuvre consists of a transition section from a linear flight path into a circular main section. In the example given here the flight velocity is held constant at 80 knots, and the side slip velocity is constrained to be zero (giving co-ordinated turns). Inverse simulations have been performed for three different right hand turns of radii 150, 200 and 250 metres. The resulting attitude and control time histories are plotted in Figure 7 as displacements from trim. The effect of severity of manoeuvre is obvious from these plots. As the radius of turn decreases, and the manoeuvre becomes more severe the required control displacements increase, and attitude

$$\begin{bmatrix} u \\ v \\ w \end{bmatrix} = \begin{bmatrix} l_1 & l_2 & l_3 \\ m_1 & m_2 & m_3 \\ n_1 & n_2 & n_3 \end{bmatrix} \begin{bmatrix} \dot{x} \\ \dot{y} \\ \dot{z} \end{bmatrix} \quad (11)$$

where l_1, \dots, n_3 are the direction cosines in the form

$$l_1 = \cos\theta \cos\psi, \quad \text{etc.}$$

The accelerations can be found by differentiating equation (10):

$$\begin{bmatrix} \ddot{u} \\ \ddot{v} \\ \ddot{w} \end{bmatrix} = \begin{bmatrix} l_1 & l_2 & l_3 \\ m_1 & m_2 & m_3 \\ n_1 & n_2 & n_3 \end{bmatrix} \begin{bmatrix} \ddot{x} \\ \ddot{y} \\ \ddot{z} \end{bmatrix} + \begin{bmatrix} \dot{l}_1 & \dot{l}_2 & \dot{l}_3 \\ \dot{m}_1 & \dot{m}_2 & \dot{m}_3 \\ \dot{n}_1 & \dot{n}_2 & \dot{n}_3 \end{bmatrix} \begin{bmatrix} \dot{x} \\ \dot{y} \\ \dot{z} \end{bmatrix} \quad (12)$$

The direction cosine rates ($\dot{l}_1, \dots, \dot{n}_3$) are functions of the attitude angles and rates in the form

$$\dot{l}_1 = -\dot{\theta} \sin\theta \cos\psi - \dot{\psi} \cos\theta \sin\psi \quad \text{etc}$$

The value of v is found from equation (5), the sideslip angle, β , being specified as a function of time throughout the manoeuvre, and since θ and ϕ are updated at each iteration, the corresponding value of ψ can be found from the second of equations (10), which on expansion becomes:

$$a \cos\psi + b \sin\psi + c = 0 \quad (13)$$

where

$$a = \dot{x} \sin\phi \sin\theta + \dot{y} \cos\phi \quad (14.1)$$

$$b = -\dot{x} \cos\phi + \dot{y} \sin\phi \sin\theta \quad (14.2)$$

$$c = \dot{z} \sin\phi \cos\theta - v \quad (14.3)$$

This equation is easily solved numerically by a Newton-Raphson method. Yaw rate is found in a similar manner from equation (12.2) and equation (7). This process is obviously not required if heading angle is constrained to a predefined function.

3.7.2 Attitude Rates and Accelerations

The attitude rates and accelerations, calculated using numerical differentiation, are needed to allow evaluation of the body axes translational and rotational velocities and accelerations. A backward difference method is used. The derivative of each attitude angle is calculated on the basis of the latest estimate of the angle, and the value at the last calculation time point. For example, pitch rate at time point k , is given by :

$$\dot{\theta}_k = \frac{\theta_k - \theta_{k-1}}{t_k - t_{k-1}} \quad (15)$$

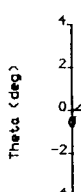
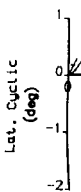
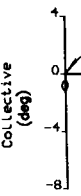
3.7.3 Body Axes Velocities and Accelerations

The body-axis translational velocities and accelerations can now be calculated using the transformation given by equations (11) and (12). The rotational velocities are calculated by manipulation of equations (3), and the rotational accelerations by differentiation of the resulting expressions. The inertial and acceleration force and moment components of the equations of motion can now be calculated.

3.7.4 The External Forces and Moments

With the body axes translational velocities all calculated, the fuselage angles of incidence may be found, from which the fuselage, tailplane and fin forces and moments may be evaluated. Using configurational data, the main rotor thrust coefficient, C_T , can be calculated from the Z-force equation (1.3 and 3.3), and the longitudinal flapping angle, β_{1c} , from the pitching moment (M) equation (1.4 and 3.4). Tail rotor thrust coefficient C_{Ttr} , and lateral flapping angle β_{1s} , are found by simultaneous solution of the remaining two (rolling and yawing) equations of motion (1.5, 1.6 and 3.5, 3.6).

The performance of the algorithm is discussed in section 5 after some results, obtained using the HELINV program, have been presented.



Fig

angle displ
most sever
case radiu
limit is re

The t
konwn resp
used to rol
collective
balancing"
intuitively
these resul

T
verificatio
solution.
manoeuvring

5.1 Verif

The
helicopter

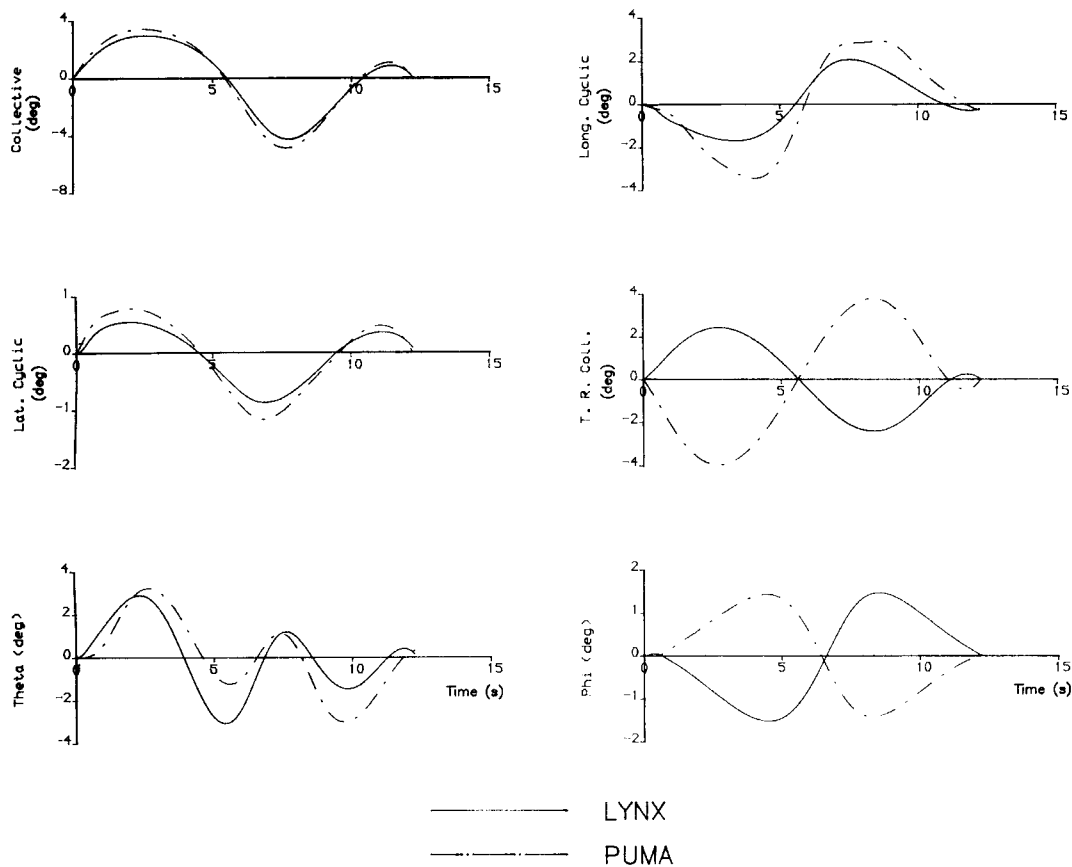


Figure 6 : Control and Attitude Time Histories From Inverse Simulation
of LYNX and PUMA Flying Hurdle-Hop Manoeuvre

$$s = 500\text{m}, h = 25\text{m}, V = 80 \text{ knots}$$

angle displacements also increase. A possible use for this comparison would be to find the most severe manoeuvre possible with a given configuration. A manoeuvre parameter (in this case radius of turn) is varied, and the control time histories monitored until a control limit is reached.

The time histories computed in this example can all be justified in the context of the known response of a real helicopter flying a similar manoeuvre. Lateral cyclic pulses are used to roll the helicopter into and out of the steady section of the turn, whilst increased collective is required to maintain constant height by overcoming the loss in "weight balancing" thrust due to disc tilt. Although the time histories generated by HELINV appear intuitively to be sensible in size and trend, it is still of importance to be able to verify these results.

5. VERIFICATION AND VALIDATION OF INVERSE TECHNIQUE

There are two stages in the evaluation of the HELINV program. The first, verification, stage confirms the accuracy of the numerical technique of the inverse solution. The second, validation, stage compares the results of inverse simulations of manoeuvring with actual flight data.

5.1 Verification of Inverse Algorithm

The HELINV program gives control angles required to fly a given flight path for a helicopter independent of pilot and control system i.e. the solutions achieved are based

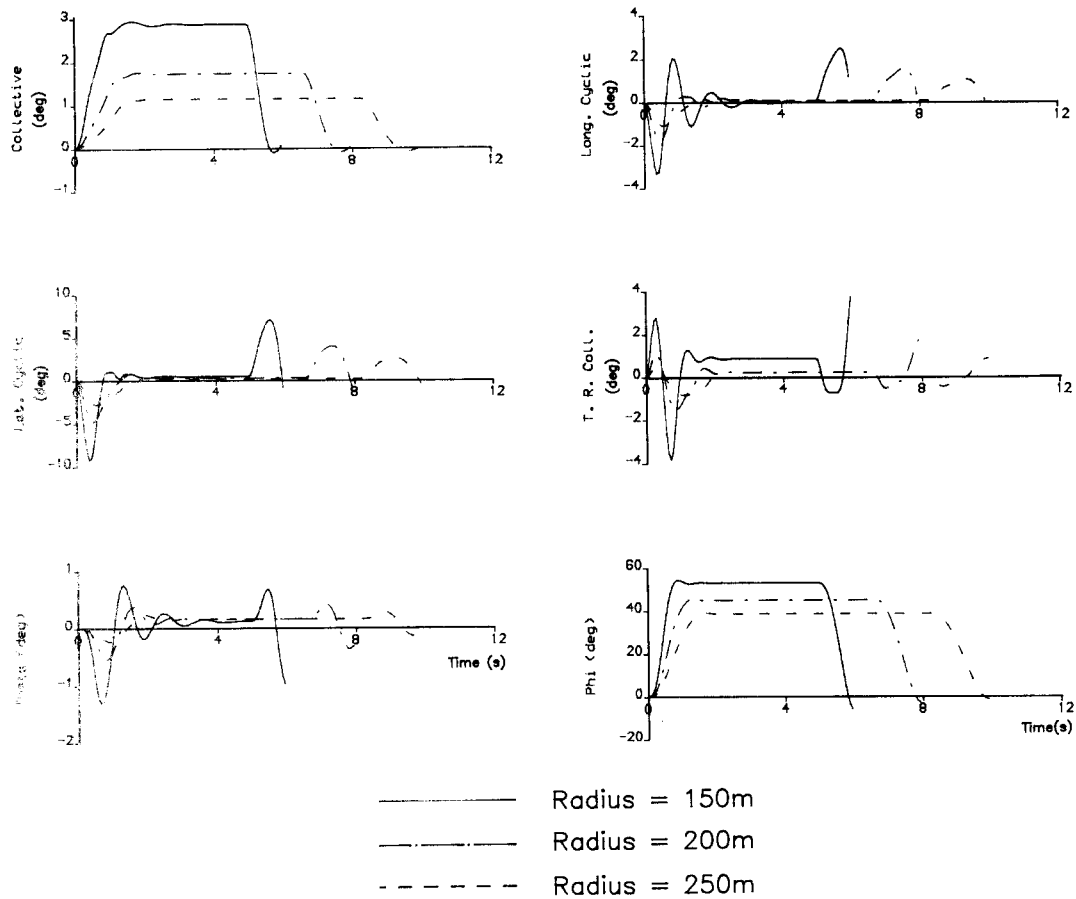


Figure 7 : Control and Attitude Time Histories from Inverse Simulation of LYNX Flying a Series of Right Hand 90 deg. Turns at a Constant Velocity of 80 knots

only on the dynamics of the aircraft. This means that any attempt to compare directly control time histories generated using the program, with actual flight data must be preceded by a verification of the inverse algorithm itself. The most appropriate method of verifying whether accurate results are being calculated is by comparison with a compatible forward simulation of the same model. This involves performing a conventional time response solution, using the mathematical model from the original HELISTAB program, to find what flight path a HELINV generated control time history produces. By comparing this control generated flight path with the commanded flight path it is possible to see how accurate the inverse method is.

The control time histories for the Puma flying the hurdle-hop manoeuvre have been used to perform a time response solution. The resulting time response flight path is compared with that demanded in the inverse solution in Figure 8. There is little difference between the two solutions in the plot of altitude variation (except a small discrepancy at the hurdle), and only a drift of 0.3m over the 500m track. This result is typical of numerous simulations taken over a wide range of conditions from which it can be concluded that the numerical algorithm is giving accurate results.

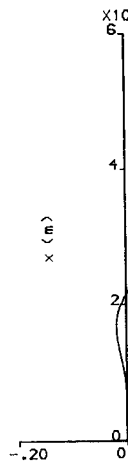


Figure 8

5.2 Validation

If u program, it strategies, measured in allows comp test. Valid being suppl agility tria prescribed m path co-ord synchronised state respon and the air therefore p simulation p control disp as the actu only seen t explicit mo consequence modified and presence of which has a second. Thi basic contro

The e Figure 9. constant hel those in the heading. W for the fid histories i inverse sim apparent the

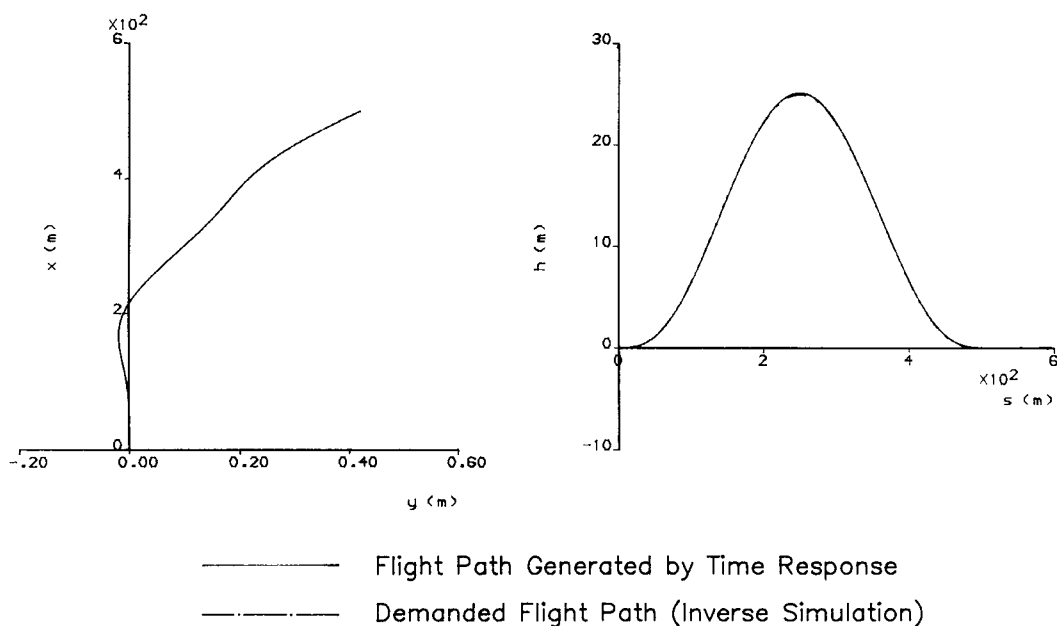


Figure 8 : Comparison Between Flight Path Demanded and that Generated by Time Response Solution Using Inverse Simulation Control Time Histories

5.2 Validation Using Flight Data from NOE Flight Trials

If useful results are to be obtained from HELINV, or any other inverse simulation program, it is important to determine the relationship between the simulated control strategies, and those adopted by pilots. It is possible to do this by using trajectories measured in flight tests to perform inverse simulations. Calculating control time histories allows comparisons between simulated control strategies and those recorded in the flight test. Validation of this sort has been performed using HELINV [12, 13], the flight data being supplied by the Royal Aerospace Establishment. The data was recorded during NOE agility trials [14, 15] at RAE Bedford where the pilot was assigned the task of flying a prescribed manoeuvre within certain performance limits. Each set of data consists of flight path co-ordinates measured at constant time increments throughout the manoeuvre, and a synchronised set of state and control time histories. The helicopter's control inputs and state responses were measured throughout the tests using a digital data acquisition system, and the aircraft's position was recorded using a kinetheodolite tracking system. It is therefore possible to take the measured flight path time histories and use the inverse simulation program, with appropriate configurational data in the model, to calculate what control displacements the simulated helicopter requires to fly precisely the same manoeuvre as the actual vehicle. Since this inverse solution is unique, the effect of the pilot is only seen through an ability to maintain a predetermined flight path and not through an explicit model of his dynamics. In this situation it has been shown [16, 17] that as a consequence of the constraints imposed on the helicopter's motion its dynamic properties are modified and oscillatory transients can be induced and persist through a manoeuvre. The presence of these oscillations causes a variation between flight data and simulation results which has a characteristic frequency, which in most cases has a period of the order of 1 second. This will be observed in the comparison discussed below and is superimposed on the basic control movements.

The example shown here is for a Lynx helicopter flying a quick-hop manoeuvre shown in Figure 9. This manoeuvre is flown from hover to hover over a specified step, maintaining constant height and heading. The constraints imposed on the pilot are therefore similar to those in the inverse simulation in which a predefined flight path must be flown with a given heading. When comparing inverse simulation and flight test results allowance must be made for the fidelity of the mathematical model used [12]. The controls and attitudes time histories in Figure 10 show comparisons between the actual flight data and that from the inverse simulation for a Lynx flying a quick-hop manoeuvre of length 300ft (91.5m). It is apparent that there is good correlation between flight test and inverse simulation for most

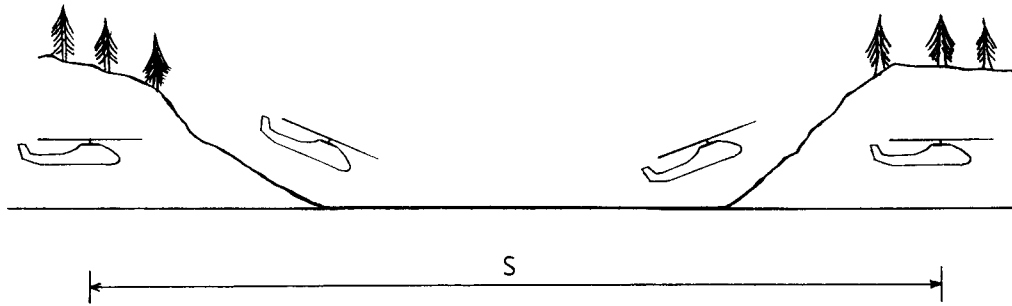


Figure 9 : The Quick Hop Manoeuvre

of the plots, small differences in the numerical values may be attributed to modelling deficiencies. The standard approach adopted by pilots flying quick-hop manoeuvres is to input initially a pulse to the longitudinal cyclic, thereby causing the rotor to tilt forward. Application of increased thrust, by increasing collective, accelerates the helicopter to a maximum velocity. This transient is then followed by a steady section, until just after midway through the manoeuvre, the direction of the thrust is reversed by a second pulse in longitudinal cyclic. During this tilting of the rotor disc, there is an interval of reduced collective. Finally, the helicopter is decelerated by increased thrust, now acting in a direction opposite to the vehicle's motion, and then, as it approaches the hover, the fuselage is brought level by a final pulse of cyclic. All of these details are visible both in the flight data and the simulation and it can be concluded that the inverse simulation calculates realistic control strategies for NOE manoeuvres. It is able to show directly how defined Mission Task Elements are able to be flown, and can give a rapid evaluation of the workload involved in flying them. Further, it is possible to investigate in a direct way how variations in the definition, such as the acceleration profile through the manoeuvre, influences the pilot task.

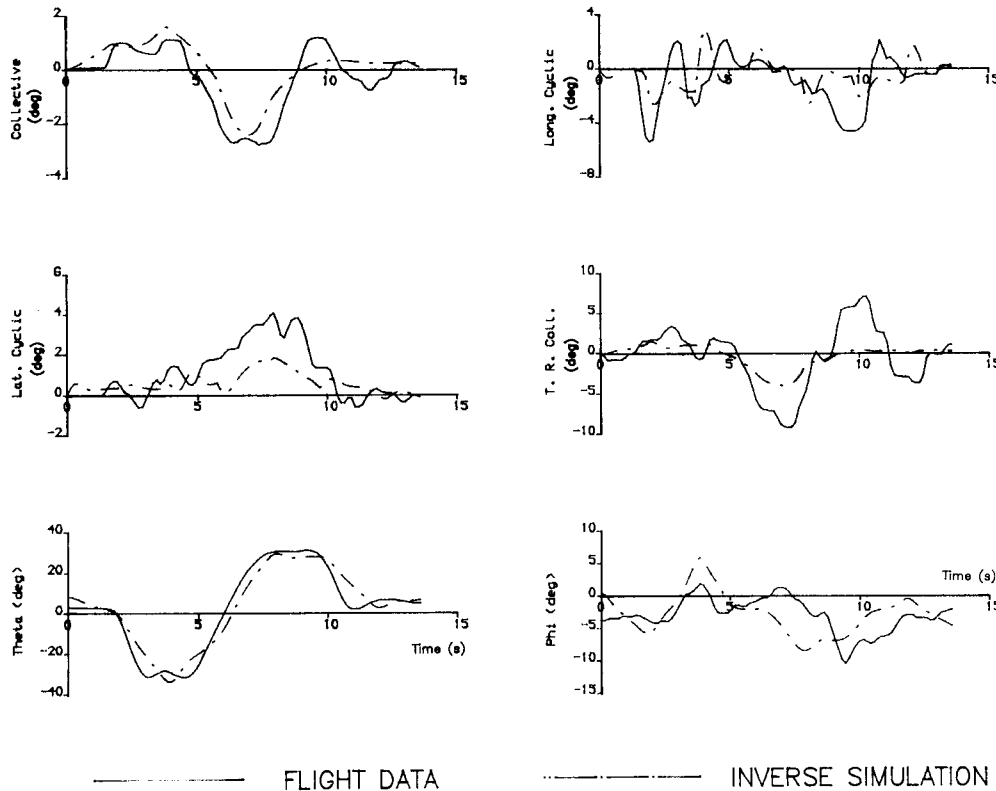


Figure 10 : Comparison of Flight Test Data and Inverse Simulation Data for LYNX Flying a 300ft. Quick-Hop Manoeuvre

The H
[8]. Agili
standard man
state and co
repetition
helicopters
controllers
that inverse
theory is of
lateral dyna

The
conditions,
low level wi
rigs) where
Helicopters
confined are
weapons deliv
in the study

1. The s
depends larg
inverse sol
approximately
Modelling imp
manoeuvre lin

2. The way
solution. I
not return t
path where t
section. Th

3. It has
a precisely
oscillations
flying the t
manoeuvres b
constrained f

4. The nu
integrity, a
modelling det

5. Despit
valid result
helicopter f
routine inve

1. D.G. Mit
Helicopt
July 198
2. B. Gmel
and Des
on Helic
3. R.H. Hoh
for Hand
Tech Rep
4. R.T. Jon
Disturbe

6. APPLICATIONS OF INVERSE SIMULATIONS

The HELINV package was originally developed for use in a study of helicopter agility [8]. Agility was quantified by studying a helicopter's performance over a series of standard manoeuvres, numerical values for an *Agility Rating* being awarded on the basis of state and control time histories for the manoeuvres. As inverse solutions allow precise repetition of manoeuvres with any number of configurations, the agility of various helicopters can be compared. Inverse solutions have found applications in the design of controllers for dynamic systems possessing highly coupled non-linearities. This implies that inverse solutions will be of use in helicopter flight mechanics where linear system theory is of limited use due to the large degree of coupling between the longitudinal and lateral dynamics of the aircraft.

The examples given in this report refer only to operations in nap-of-the-earth conditions, but there are other areas where helicopters have to manoeuvre close to obstacles at low level with precision. For example, operations from offshore platforms (ships and oil rigs) where the helicopter has to take off and land close to a super-structure. Helicopters in "commando" type operations also have to take off and land rapidly within confined areas. Other possible applicable tasks might be air-to-air combat or preset weapons delivery manoeuvres. The inverse method presented in this paper could prove useful in the study of helicopter performance in all of these areas.

7. CONCLUSIONS

1. The severity of manoeuvre for which it is possible to calculate inverse solutions depends largely on the limitations of the mathematical model. The current simulation allows inverse solutions to be found for manoeuvres with maximum normal load factors of approximately 2.2g for purely turning manoeuvres, and 1.7g for longitudinal flight. Modelling improvements, such as the inclusion of rotor degrees of freedom, should see these manoeuvre limits extended.
2. The way in which flight paths are modelled has consequences on the form of the inverse solution. It is noticeable from Figure 7 that the attitude and control time histories do not return to their commanded trim values. This is due to a discontinuity in the flight path where the analytical function defining the flight path joins the straight line trim section. This small error grows as the manoeuvres become more severe.
3. It has been shown [16, 17] that as a consequence of constraining the helicopter to fly a precisely defined manoeuvre its dynamic properties are modified, and constraint induced oscillations appear. These oscillations are visible in the time histories for the Lynx flying the turn manoeuvres (Fig. 7). These oscillations become more pronounced as the manoeuvres become more severe. This effect can often be observed in real helicopters during constrained flight [13].
4. The numerical algorithm has been thoroughly validated both in terms of its numerical integrity, and also in its ability to produce realistic results notwithstanding minor modelling deficiencies.
5. Despite these minor problems and limitations, the HELINV package produces useful and valid results. Its success is due to a solution method which exploits a knowledge of helicopter flight mechanics and which is sufficiently fast to make inverse solutions a routine investigative tool.

8. REFERENCES

1. D.G. Mitchell, R.H. Hoh, A. Atencio, Jr., "Classification of Response-Types for Attack Helicopter Combat Tasks", *Journal of the American Helicopter Society*, Vol. 33, No. 3, July 1988.
2. B. Gmelin, H.-J. Pausder, "Test Techniques for Helicopter Handling Qualities Evaluation and Design", *Proceedings of the Royal Aeronautical Society International Conference on Helicopter Handling Qualities and Control*, London, November 1988.
3. R.H. Hoh, D.F. Mitchell, D.L. Aponso, D.L. Key, C.L. Blanken, "Proposed Specification for Handling Qualities of Military Rotorcraft. Vol. 1 - Requirements", USAAVSCOM Tech Report 87-A-4, May 1988.
4. R.T. Jones, "A Simplified Application of the Method of Operators to the Calculation of Disturbed Motions of an Airplane", *NACA TR 560*, 1936.

5. G. Meyer, L. Cicolani, "Application of Nonlinear Systems Inverses to Automatic Flight Control Systems Design", Paper No. 10, *Theory and Applications of Optimal Control in Aerospace Systems*, AGARDograph 251, 1981.
6. O. Kato, I. Sugiura, "An Interpretation of Airplane General Motion and Control as Inverse Problem", *Journal of Guidance and Control*, Vol. 9, No. 2, June 1986.
7. S.S. Houston, A.E. Caldwell, "A Computer Based Study of Helicopter Agility, Including the Influence of an Active Tailplane", Paper No. 70, Proceedings of the 10th European Rotorcraft Forum, The Hague, Sept. 1984.
8. D.G. Thomson, "Evaluation of Helicopter Agility Through Inverse Solution of the Equations of Motion", Ph.D. Thesis, Department of Aeronautics and Fluid Mechanics, University of Glasgow, June 1987.
9. H.C. Curtiss, Jr., G. Price, "Studies of Rotorcraft Agility and Maneuverability", Paper No. 69, Proceedings of the 10th European Rotorcraft Forum, The Hague, Sept. 1984.
10. G.D. Padfield, "A Theoretical Model of Helicopter Flight Mechanics for Application to Piloted Simulation", RAE TR 81048, Apr. 1981.
11. D.G. Thomson, R. Bradley, "Mathematical Representation of Manoeuvres Commonly Found in Helicopter Nap-of-the-Earth Flight", University of Glasgow, Dept. of Aeronautics and Fluid Mechanics, Internal Report 8801, Feb. 1988
12. D.G. Thomson, R. Bradley, "Validation of Helicopter Mathematical Models by Comparison of Data from Nap-of-the-Earth Flight Tests and Inverse Simulations", Paper No. 87, Proceedings of the 14th European Rotorcraft Forum, Milan, Italy, September 1988.
13. D.G. Thomson, R. Bradley, "An Investigation of Pilot Strategy in Helicopter Nap-of-the-Earth Manoeuvres by Comparison of Flight Data and Inverse Simulations", Proceedings of the Royal Aeronautical Society International Conference on Helicopter Handling Qualities and Control, London, November 1988.
14. M.T. Charlton, G.D. Padfield, Lt. Cdr. R. I. Horton, "Helicopter Agility in Low Speed Manoeuvres", Paper No. 9.10, Proceedings of the 13th European Rotorcraft Forum, Arles, France, September 1987.
15. G.D. Padfield, M.T. Charlton, "Aspects of RAE Flight Research into Helicopter Agility and Pilot Control Strategy", Proceedings of the Helicopter Handling Qualities Specialists Meeting, AMES Research Center, Moffat Field, June 1986.
16. D.G. Thomson, R. Bradley, "An Investigation of the Stability of Flight Path Constrained Manoeuvres by Inverse Simulation", Paper No.7.7, Proceedings of the 13th European Rotorcraft Forum, Arles, France, September 1987.
17. D.G. Thomson, R. Bradley, "Inverse Solution of the Helicopter Linearised Equations of Motion", University of Glasgow, Dept. of Aeronautics and Fluid Mechanics, Internal Report 8707, Dec. 1987.

10. ACKNOWLEDGEMENTS

The authors would like to acknowledge the contribution of Dr G.D. Padfield of the Royal Aerospace Establishment, Bedford to this work, particularly in relation to the HELISTAB model. Thanks are also due to Mr M.T. Charlton of RAE Bedford for his assistance in preparing the flight data used. This research was funded as part of the Ministry of Defence Research Agreement 2048/39/XR/FS. Work in this field is currently funded by the Royal Society under their University Research Fellowship scheme.